



1 **An intercomparison of oceanic methane and nitrous oxide measurements**

2

3 Samuel T. Wilson^{1*}, Hermann W. Bange², Damian L. Arévalo-Martínez², Jonathan Barnes³,
4 Alberto V. Borges⁴, Ian Brown⁵, John L. Bullister⁶, Macarena Burgos⁷, David W. Capelle⁸,
5 Michael Casso⁹, Mercedes de la Paz^{10†}, Laura Farías¹¹, Lindsay Fenwick⁸, Sara Ferrón¹, Gerardo
6 Garcia¹¹, Michael Glockzin¹², David M. Karl¹, Annette Kock², Sarah Laperriere¹³, Cliff S.
7 Law^{14,15}, Cara C. Manning⁸, Andrew Marriner¹⁴, Jukka-Pekka Myllykangas¹⁶, John W.
8 Pohlman⁹, Andrew P. Rees⁵, Alyson E. Santoro¹³, Mabel Torres¹¹, Philippe D. Tortell⁸, Robert
9 C. Upstill-Goddard³, David P. Wisegarver⁶, Guiling L. Zhang¹⁷, Gregor Rehder¹²

10

11 ¹University of Hawai'i, Daniel K. Inouye Center for Microbial Oceanography: Research and
12 Education (C-MORE), Honolulu, Hawai'i, USA

13 ²GEOMAR Helmholtz Centre for Ocean Research Kiel, Düsternbrooker Weg 20 24105 Kiel,
14 Germany

15 ³Newcastle University, School of Natural and Environmental Sciences, Newcastle upon Tyne,
16 UK

17 ⁴Université de Liège, Unité d'Océanographie Chimique, Liège, Belgium

18 ⁵Plymouth Marine Laboratory, Plymouth, UK

19 ⁶National Oceanic and Atmospheric Administration, Pacific Marine Environmental Laboratory,
20 Seattle, Washington, USA

21 ⁷Universidad de Cádiz, Instituto de Investigaciones Marinas, Departamento Química-Física
22 Cádiz, Spain

23 ⁸University of British Columbia, Vancouver, Department of Earth, Ocean and Atmospheric
24 Sciences, British Columbia, Canada

25 ⁹US Geological Survey, Woods Hole Coastal and Marine Science Center, Woods Hole, USA

26 ¹⁰Instituto de Investigaciones Marinas, Vigo, Spain

27 ¹¹University of Concepción, Department of Oceanography, Laboratory of Oceanographic
28 Process and Climate (PROFC), Concepción, Chile

29 ¹²Leibniz Institute for Baltic Sea Research Warnemünde, Rostock, Germany

30 ¹³University of California Santa Barbara, Department of Ecology, Evolution, and Marine
31 Biology, Santa Barbara, USA

32 ¹⁴National Institute of Water and Atmospheric Research (NIWA), Wellington, New Zealand



33 ¹⁵Department of Chemistry, University of Otago, Dunedin, New Zealand

34 ¹⁶University of Helsinki, Department of Environmental Sciences, Helsinki, Finland

35 ¹⁷Ocean University of China, Department of Marine Chemistry, Qingdao, China

36

37 †Current address: Instituto Español de Oceanografía, Centro Oceanográfico de A Coruña, A

38 Coruña, Spain

39

40 *corresponding author: stwilson@hawaii.edu



41 **Abstract.** Large scale climatic forcing is impacting oceanic biogeochemical cycles and is
42 expected to influence the water-column distribution of trace gases including methane and nitrous
43 oxide. Our ability as a scientific community to evaluate changes in the water-column inventories
44 of methane and nitrous oxide depends largely on our capacity to obtain robust and accurate
45 concentration measurements which can be validated across different laboratory groups. This
46 study represents the first formal, international, intercomparison of oceanic methane and nitrous
47 oxide measurements whereby participating laboratories received batches of seawater samples
48 from the subtropical Pacific and the Baltic Sea. Additionally, compressed gas standards from the
49 same calibration scale were distributed to the majority of participating laboratories to improve
50 the analytical accuracy of the gas measurements. The computations used by each laboratory to
51 derive the dissolved gas concentrations were also evaluated for inconsistencies (*e.g.* pressure and
52 temperature corrections, solubility constants). The results from the intercomparison and
53 intercalibration exercises provided invaluable insights into methane and nitrous oxide
54 measurements. It was observed that analyses of seawater samples with the lowest concentrations
55 of methane and nitrous oxide had the lowest precisions. In comparison, while the analytical
56 precision for samples with the highest concentrations of trace gases was better, the variability
57 between the different laboratories was higher; 36% for methane and 27% for nitrous oxide. In
58 addition, the comparison of different batches of seawater samples with methane and nitrous
59 oxide concentrations that ranged over an order of magnitude revealed the ramifications of
60 different calibration procedures for each trace gas. Overall, this paper builds upon the
61 intercomparison results to develop a framework for improving oceanic methane and nitrous
62 oxide measurements, with the aim of precluding future analytical discrepancies between
63 laboratories.



64 1. Introduction

65 The increasing mole fractions of greenhouse gases in the Earth's atmosphere are causing long-
66 term climate change with unknown future consequences. Two greenhouse gases, methane and
67 nitrous oxide, together contribute approximately 23% of total radiative forcing attributed to well-
68 mixed greenhouse gases (Myhre et al., 2013). It is imperative that the monitoring of methane
69 and nitrous oxide in the Earth's atmosphere is accompanied by measurements at the Earth's
70 surface to better inform the sources and sinks of these climatically important trace gases. This
71 includes measurements of dissolved methane and nitrous oxide in the marine environment,
72 which is an overall source of both gases to the overlying atmosphere (Nevison et al., 1995;
73 Anderson et al., 2010; Naqvi et al., 2010; Freing et al., 2012; Ciais et al., 2014).

74 Oceanic measurements of methane and nitrous oxide are conducted as part of established
75 time-series locations, along hydrographic survey lines, and during disparate oceanographic
76 expeditions. Within low to mid-latitude regions of the open ocean, the surface waters are
77 typically slightly super-saturated with respect to atmospheric equilibrium for both methane and
78 nitrous oxide. There is typically an order of magnitude range in concentration along a vertical
79 water-column profile at any particular open ocean location (e.g. Wilson et al., 2017). In contrast
80 to the open ocean, near-shore environments, which are subject to river inputs, coastal upwelling,
81 benthic exchange and other processes, have higher concentrations and greater spatial and
82 temporal heterogeneity (e.g. Schmale et al., 2010; Upstill-Goddard and Barnes, 2016).

83 Methods for quantifying dissolved methane and nitrous oxide have evolved and somewhat
84 diverged since the first measurements were made in the 1960s (Craig and Gordon 1963;
85 Atkinson and Richards 1967). Some laboratories employ purge-and-trap methods for extracting
86 and concentrating the gases prior to their analysis (e.g. Zhang et al., 2004; Bullister and
87 Wisegarver, 2008; Capelle et al., 2015; Wilson et al., 2017). Others equilibrate a seawater
88 sample with an overlying headspace gas and inject a fixed volume of the gaseous phase into a
89 gas analyzer (e.g. Upstill-Goddard et al., 1996; Walter et al., 2005; Farias et al., 2009).
90 Additional developments for continuous underway surface seawater measurements use
91 equilibrators systems of various designs coupled to a variety of detectors (e.g. Weiss et al., 1992;
92 Butler et al., 1989; Güllow et al., 2011; Arévalo-Martínez et al., 2013). Determining the level
93 of analytical comparability between different laboratories for discrete samples of methane and
94 nitrous oxide is an important step towards improved comprehensive global assessments. Such



95 intercomparison exercises are critical to determining the spatial and temporal variability of
96 methane and nitrous oxide across the world oceans with confidence, since no single laboratory
97 can single-handedly provide all the required measurements at sufficient resolution. Previous
98 comparative exercises have been conducted for other trace gases *e.g.* carbon dioxide,
99 dimethylsulphide, and sulfur hexafluoride (Dickson et al., 2007; Bullister and Tanhua, 2010;
100 Swan et al., 2014) and for trace elements (Cutter et al., 2013). These exercises confirm the value
101 of the intercomparison concept.

102 To instigate this process for methane and nitrous oxide, a series of international
103 intercomparison exercises were conducted between 2013 and 2017, under the auspices of
104 Working Group #143 of the Scientific Committee on Oceanic Research (SCOR) ([www.scor-](http://www.scor-int.org)
105 [int.org](http://www.scor-int.org)). Discrete seawater samples collected from the subtropical Pacific Ocean and the Baltic
106 Sea were distributed to the participating laboratories (Table 1). The samples were selected to
107 cover a representative range of concentrations across marine locations, from the oligotrophic
108 open ocean to highly productive waters, and in some instances sub-oxic, coastal waters. An
109 integral component of the intercomparison exercise was the production and distribution of
110 methane and nitrous oxide gas standards to members of the SCOR Working Group. The
111 intercomparison exercise was conceived and evaluated with the following four questions in
112 mind:

113 Q1. What is the agreement between the SCOR gas standards and the ‘in-house’ gas standards
114 used by each laboratory?

115 Q2. How do measured values of dissolved methane and nitrous oxide compare across
116 laboratories?

117 Q3. Despite the use of different analytical systems, are there general recommendations to reduce
118 uncertainty in the accuracy and precision of methane and nitrous oxide measurements?

119 Q4. What are the implications of inter-laboratory differences for determining the spatial and
120 temporal variability of methane and nitrous oxide in the oceans?

121

122 **2. Methods**

123 **2.1 Calibration of nitrous oxide and methane using compressed gas standards**

124 Laboratory-based measurements of oceanic methane and nitrous oxide require separation of the
125 dissolved gas from the aqueous phase, with the analysis conducted on the gaseous phase.



126 Calibration of the analytical instrumentation used to quantify the concentration of methane and
127 nitrous oxide is nearly always conducted using compressed gas standards, the specifics of which
128 vary between each laboratory. Therefore, the reporting of methane and nitrous oxide datasets
129 ought to be accompanied by a description of the standards used, including their methane and
130 nitrous oxide mole fractions, the declared accuracies, and the composition of their balance or
131 ‘make-up’ gas. For both gases, the highest accuracy commercially available standards have
132 mole fractions close to current day atmospheric values. These standards can be obtained from
133 national agencies e.g. National Oceanic and Atmospheric Administration Global Monitoring
134 Division (NOAA GMD), the National Institute of Metrology China, and the Central Analytical
135 Laboratories of the European Integrated Carbon Observation System Research Infrastructure
136 (ICOS-RI). By comparison, it is more difficult to obtain highly accurate methane and nitrous
137 oxide gas standards with mole fractions exceeding modern-day atmospheric values. This is
138 particularly problematic for nitrous oxide due to the nonlinearity of the widely used Electron
139 Capture Detector (ECD) (Butler and Elkins, 1991).

140 The absence of a widely available high mole fraction, high accuracy nitrous oxide gas
141 standard was noted as a primary concern at the outset of the intercomparison exercise.
142 Therefore, a set of high-pressure primary gas standards was prepared for the SCOR Working
143 Group by John Bullister and David Wisegarver at NOAA Pacific Marine and Environmental
144 Laboratory (PMEL). One batch, referred to as Air Ratio Standard (ARS), had methane and
145 nitrous oxide mole fractions similar to modern air and the other batch, referred to as Water Ratio
146 Standard (WRS) had higher methane and nitrous oxide mole fractions for calibration of high
147 concentration water samples. These SCOR primary standards were checked for stability over a
148 12 month period and assigned mole fractions on the same calibration scale, known as ‘SCOR-
149 2016.’ A comparison was conducted with NOAA standards prepared on the SIO98 calibration
150 scale for nitrous oxide and the NOAA04 calibration scale for methane. Based on the comparison
151 with NOAA standards, the uncertainty of the methane and nitrous oxide mole fractions in the
152 ARS and the uncertainty of the methane mole fraction in the WRS were all estimated at better
153 than 1%. By contrast, the uncertainty of the nitrous oxide mole fraction in the WRS was
154 estimated at 2-3%. The gas standards were distributed to twelve of the laboratories involved in
155 this study (Table 1). A technical report on the production of the gas standards and their assigned
156 absolute mole fractions is available at www.scor-int.org/SCOR_Publications.



157

158 **2.2 Collection of discrete samples of nitrous oxide and methane**

159 Dissolved methane and nitrous oxide samples for the intercomparison exercise were collected
160 from the subtropical Pacific Ocean and the Baltic Sea. Pacific samples were obtained on 28
161 November 2013 and 24 February 2017 from the Hawaii Ocean Time-series (HOT) long-term
162 monitoring site, Station ALOHA, located at 22.75 N, 158.00 W. The November 2013 samples
163 are included in Figure S1 and S2 in the Supplement, but are not discussed in the main Results or
164 Discussion because fewer laboratories were involved in the initial intercomparison, and the
165 results from these samples support the same conclusions obtained with the more recent sample
166 collections. Seawater was collected using Niskin-like bottles designed by John Bullister (NOAA
167 PMEL), which help minimize contamination of trace gases, in particular chlorofluorocarbons
168 and sulfur hexafluoride (Bullister and Wisegarver, 2008). The bottles were attached to a rosette
169 with a conductivity-temperature-depth (CTD) package. Seawater was collected from two depths:
170 700 m and 25 m, where the near-maximum and minimum water-column concentrations for
171 methane and nitrous oxide at this location can be found. Replicate samples were collected from
172 each bottle, with one replicate reserved for analysis at the University of Hawaii to evaluate
173 variability between sampling bottles. Seawater was dispensed from the Niskin-like bottles using
174 Tygon® tubing into the bottom of borosilicate glass bottles, allowing overflow of at least two
175 sample volumes and ensuring the absence of bubbles. Most sample bottles were 240 mL in size
176 and were sealed with no headspace using butyl-rubber stoppers and aluminum crimp-seals. A
177 few laboratory groups requested smaller crimp-sealed glass bottles ranging from 20-120 mL in
178 volume and two laboratories used 1 L glass bottles which were closed with a stopper and sealed
179 with Apiezon® grease. Seawater samples were collected in quadruplicate for each laboratory.
180 All samples were preserved using saturated mercuric chloride solution (100 µL of saturated
181 mercuric chloride solution per 100 mL of seawater sample) and stored in the dark at room
182 temperature until shipment.

183 Samples from the western Baltic Sea were collected during 15-21 October 2016, onboard the
184 R/V *Elisabeth Mann Borgese* (Table 2). Since the Baltic Sea consists of different basins with
185 varying concentrations of oxygen beneath permanent haloclines (Schmale et al., 2010), a larger
186 range of water-column methane and nitrous oxide concentrations were accessible for inter-
187 laboratory comparison compared to Station ALOHA. For all seven Baltic Sea stations, the



188 water-column was sampled into an on-deck 1,000 L water tank that was subsequently
189 subsampled into discrete sample bottles. At three stations (BAL1, BAL3, and BAL6), the water
190 tank was filled from the shipboard high-throughput underway seawater system. For deeper
191 water-column sampling at the stations BAL2, BAL4, and BAL5, the water tank was filled using
192 a pumping CTD system (Strady et al., 2008) with a flow rate of 6 L min⁻¹ and a total pumping
193 time of approximately 3 h. For the final deep water-column station, BAL7, the pump that
194 supplied the shipboard underway system was lowered to a depth of 21 m to facilitate a shorter
195 pumping time of approximately 20 mins. Subsampling the water tank for all samples took
196 approximately 1 h in total and the total sampling volume was less than 100 L. To verify the
197 homogeneity of the seawater during the sampling process, the first and last samples collected
198 from the water tank were analyzed by Newcastle University onboard the research vessel. In
199 contrast to the Pacific Ocean sampling, which predominantly used 240 mL glass vials, each
200 laboratory provided their own preferred vials and stoppers for the Baltic Sea samples. Seawater
201 samples were collected in triplicate for each laboratory. All samples were preserved with 100
202 µL of saturated mercuric chloride solution per 100 ml of seawater sample, with the exception of
203 samples collected by U.S. Geological Survey, who analyzed unpreserved samples onboard the
204 research vessel.

205

206 **2.3. Sample analysis**

207 Each laboratory measured dissolved methane and nitrous oxide slightly differently. A full
208 description of each laboratory's method is not included in the main document and instead can be
209 found in Table S6 and Table S7 in the Supplement for methane and nitrous oxide, respectively.

210 The majority of laboratories measured methane and nitrous oxide by equilibrating the
211 seawater sample with an overlying headspace and subsequently injecting a portion of the gaseous
212 phase into the gas analyzer. This method has been conducted since the 1960s when gas
213 chromatography was first used to quantify dissolved hydrocarbons (McAuliffe, 1963). The
214 headspace was created using helium, nitrogen, or high-purity air to displace a portion of the
215 seawater sample within the sample bottle. Alternatively, a subsample of the seawater was
216 transferred to a gas-tight syringe and the headspace gas subsequently added. The volume of the
217 vessel used to conduct the headspace equilibration ranged from 20 ml borosilicate glass vials to 1
218 L glass vials and syringes used by Newcastle University and U.S. Geological Survey,



219 respectively. The dissolved gases equilibrated with the overlying headspace at a controlled
220 temperature for a set period of time that ranged from 20 min to 24 h. The equilibration process
221 was typically enhanced by some initial period of physical agitation. After equilibration, an
222 aliquot of the headspace was transferred into the gas analyzer (GA) by either physical injection,
223 displacement using a brine solution, or injection using a switching valve. Alternatively, a
224 subsample of the headspace was collected into a gas tight syringe and subsequently injected into
225 the GA. Some laboratories incorporated a drying agent and a carbon dioxide scrubber prior to
226 analysis. The gas sample passed through a multi-port injection valve containing a sample loop of
227 known volume, which transferred the gas sample directly onto the analytical column within the
228 oven of the GA. Calibration of the instrument was achieved by passing the gas standards
229 through the injection valve.

230 The final gas concentrations using the headspace equilibration method was calculated by:

231

$$232 \quad [1] \quad C_{gas} [\text{nmol L}^{-1}] = \left(\beta x P V_{wp} + \frac{xP}{RT} V_{hs} \right) / V_{wp}$$

233

234 where β is the Bunsen solubility of nitrous oxide (Weiss and Price, 1980) or methane
235 (Wiesenburg and Guinasso, 1979) in $\text{nmol L}^{-1} \text{atm}^{-1}$, x is the dry gas mole fraction (ppb)
236 measured in the headspace, P is the atmospheric pressure (atm), V_{wp} is the volume of water
237 sample (mL), V_{hs} is the volume (mL) of the created headspace, R is the gas constant (0.08205746
238 $\text{L atm K}^{-1} \text{mol}^{-1}$), and T is equilibration temperature in Kelvin (K). An example calculation is
239 provided in Table S8 in the Supplement.

240 In contrast to the headspace equilibrium method, five laboratories used a purge-and-trap
241 system for methane and/or nitrous oxide analysis (Table S6 and Table S7 in the Supplement).
242 These systems were directly coupled to a Flame Ionization Detector (FID) or ECD, with the
243 exception of University of British Columbia, where a quadrupole mass spectrometer with an
244 electron impact ion source and Faraday cup detector were used (Capelle et al., 2015). The
245 purge-and-trap systems were broadly similar, each transferring the seawater sample to a sparging
246 chamber. Sparging times typically ranged from 5-10 min and the sparge gas was either high
247 purity helium or high purity nitrogen. Further purification of the sparge gas was achieved prior
248 to use by passing it through tubing packed with Poropak Q and maintained at low temperatures.
249 This is a requirement to achieve a low blank signal. The elutant gas was dried using Nafion or



250 Drierite, and subsequently cryotrapped on a sample loop packed with Porapak Q to aid retention
251 of methane and nitrous oxide. Cryotrapping was achieved using liquid nitrogen (-165°C) or
252 cooled ethanol (-70°C). Subsequently, the valve was switched to inject mode and the sample
253 loop was rapidly heated to transfer its contents onto the analytical column. Calibration was
254 achieved by injecting standards via sample loops using multi-port injection valves. Injection of
255 standards prior to the sparging chamber allowed for calibration of the purge-and-trap gas
256 handling system, in addition to the GA. Calculation of the gas concentrations using the purge-
257 and-trap method was achieved by application of the ideal gas law to the standard gas
258 measurements:

$$259 \quad [2] \quad PV = nRT$$

260 where P , R , and T are the same as Equation 1, V represents the volume of gas injected (L),
261 and n represents moles of gas injected. Rearranging Equation 2 yields the number of moles of
262 methane or nitrous oxide gas for each sample loop injection of compressed gas standards. These
263 values were used to derive a calibration curve based on the measured peak areas of the injected
264 standards, in order to derive the number of moles measured for each unknown sample. To
265 calculate concentrations of methane or nitrous oxide in a water sample, the number of moles
266 measured were divided by the volume (L) of seawater sample analyzed. An example calculation
267 is provided in Table S8 in the Supplement.

268

269 **2.4 Data analysis**

270 The final concentrations of methane and nitrous oxide are reported in nmol kg^{-1} . The analytical
271 precision for each batch of samples obtained by each of the individual laboratories was estimated
272 from the analysis of replicate seawater samples and reported as the coefficient of variation (%).
273 The values reported by each laboratory for all the batches of seawater samples are shown in
274 Tables S1 to S4 in the Supplement. Due to the observed inter-laboratory variability, it is likely
275 that the median value of methane and nitrous oxide for each batch of samples does not represent
276 the absolute *in situ* concentration. As this complicates the analytical accuracy for each
277 laboratory, we instead calculated the percentage difference between the median concentration
278 determined for each set of samples and the mean value reported by an individual laboratory. The
279 presence of outliers was established using the Interquartile Range (IQR) and by comparing with
280 one standard deviation applied to the overall median value.



281

282 3. Results

283 3.1 Comparison of methane and nitrous oxide gas standards

284 Six laboratories compared their existing ‘in-house’ standards of methane with the SCOR
285 standards. This was done by calibrating in-house standards and deriving a mixing ratio for the
286 SCOR standards which were treated as unknowns. Four laboratories reported methane values for
287 either the ARS or WRS within 3% of their absolute concentration, whereas two laboratories
288 reported an offset of 6% and 10% between their in-house standards and the SCOR standards
289 (Table S6 in the Supplement). For those laboratories who measured the SCOR standards to
290 within 3% or better accuracy, observed offsets in methane concentrations from the overall
291 median cannot be due to the calibration gas.

292 Seven laboratories compared their own in-house standards of nitrous oxide with the prepared
293 SCOR standards. Six laboratories reported values of nitrous oxide for the ARS which were
294 within 3% of the absolute concentration, with the remaining laboratory reporting an offset of
295 10% (Table S7 in the Supplement). The majority of these laboratories (five out of six groups)
296 compared the SCOR ARS with NOAA GMD standards, which have a balance gas of air instead
297 of nitrogen. Some laboratories with analytical systems that incorporated fixed sample loops (*e.g.*
298 1 or 2 ml loops housed in a 6-port or 10-port injection valve) had difficulty analyzing the WRS,
299 as the peak areas created by the high mole fraction of the standard exceeded the signal typically
300 measured from in-house standards or acquired by sample analysis, by an order of magnitude.
301 The high mole fraction of the WRS was not an issue when multiple sample loops of varying
302 sizes were incorporated into the analytical system, which was the case for purge-and-trap based
303 designs. For the two laboratories which had comparable values of their in-house standard and
304 the WRS, an offset of 3% and a >20% offset was reported.

305

306 3.2 Methane concentrations in the intercomparison samples

307 Overall, median methane concentrations in seawater samples collected from the Pacific
308 Ocean and the Baltic Sea ranged from 0.9 to 60.3 nmol kg⁻¹ (Table 2). Out of 101 reported
309 values, 3 outliers were identified using the IQR criterion and were not included in further
310 analysis. The methane data values for each batch of samples analyzed by each laboratory,



311 including the mean and standard deviation, the number of samples analyzed, and the % offset
312 from the overall median value are reported in Table S1 and Table S2 in the Supplement.

313 The two Pacific Ocean sampling sites had the lowest water-column concentrations of
314 methane (Fig. 1a and 1b). The PAC1 samples collected from within the mesopelagic zone,
315 where methane concentrations have been reported to be less than 1 nmol kg⁻¹ (Reeburgh et al.,
316 2007; Wilson et al., 2017), showed a distribution of reported concentrations skewed towards the
317 higher values. For the PAC1 samples, 7 out of 12 laboratories reported values ≤1 nmol kg⁻¹ and
318 the mean coefficient of variation for all laboratories was 11% (Table 2). In contrast to the
319 mesopelagic samples, the methane concentrations for the near-surface seawater samples (PAC2)
320 were close to atmospheric equilibrium (Fig. 1b). Measured concentrations of methane for PAC2
321 samples ranged from 1.9 to 3.8 nmol kg⁻¹ and the mean coefficient of variation for all
322 laboratories was 7%. Similar to the PAC1 samples, PAC2 also had a distribution of data skewed
323 towards the higher concentrations.

324 Three Baltic Sea sampling sites (BAL1, BAL3, and BAL6) had median methane
325 concentrations that ranged from 4.1 to 5.7 nmol kg⁻¹ (Fig. 1c). The BAL1 samples also showed a
326 skewed distribution of reported values towards higher concentrations, as seen in PAC1 and
327 PAC2 samples. However, this was not evident in BAL3 or BAL6, which have a higher
328 agreement between the reported methane concentrations. For these three sets of Baltic Sea
329 samples, the mean coefficient of variation for all laboratories ranged from 4% (BAL3) to 9%
330 (BAL1). The next three Baltic Sea samples (BAL4, BAL5, and BAL7) had methane
331 concentrations that ranged from 18.8 to 35.4 nmol kg⁻¹ (Fig. 1d). These three sets of samples
332 had a normal distribution of data and the highest agreement between the reported concentrations
333 for all of the Pacific Ocean and Baltic Sea samples. Furthermore, for these three sets of samples,
334 the mean coefficient of variation for all laboratories was 4% (Table 2). The final Baltic Sea
335 sample (BAL2) had the highest concentrations of methane, with a median reported value of 60.3
336 nmol kg⁻¹, and a large range of values (45.2 to 67.2 nmol kg⁻¹; Fig. 1e). The BAL2 samples had
337 the lowest overall mean coefficient of variation for all laboratories; 2% (Table 2).

338 Further analysis of the data was conducted to better comprehend the factors that caused the
339 observed inter-laboratory variability in methane measurements. The deviation from median
340 values was calculated for each sample collected from the Baltic Sea (Fig. 2). The Pacific Ocean
341 samples (PAC1 and PAC2) were not included in this analysis due to the skewed distribution of



342 data. There were also some instances in the Baltic Sea samples, where the median concentration
343 might not have realistically represented the absolute *in situ* methane concentration. This was
344 most likely to have occurred at low concentrations due to the skewed distribution of reported
345 concentrations (*e.g.* BAL1) or at high concentrations where there was a large range in reported
346 values (*e.g.* BAL2). The results revealed that a few laboratories (Datasets D, F, and G) were
347 consistently within or close to 5% of the median value for all batches of seawater samples (Fig.
348 2). Some laboratories (*e.g.* Datasets B, C, and H) had a higher deviation from the median value
349 at higher methane concentrations. Two laboratories (Datasets J and K) had a higher deviation
350 from the median value at lower methane concentrations. Finally, in some cases it was not
351 possible to determine a trend (Datasets A and E), due to the variability.

352 The reasons behind the trends for each dataset became more apparent when considering the
353 response of the FID at nanomolar concentrations of methane and a ‘typical’ calibration curve
354 (Fig. 3). The FID has a linear response to methane at nanomolar values and therefore a high
355 level of accuracy across a relatively wide range of *in situ* methane concentrations can be
356 obtained with the correct slope and intercept. To demonstrate this, calibration curves for
357 methane were provided by the University of Hawaii. These revealed minimal variation in the
358 slope value when calibration points were increased from low mole fractions (Fig. 3a) to higher
359 mole fractions (Fig. 3b). However, the intercept value was sensitive to the range of calibration
360 values used, and this effect was further exacerbated when only the higher calibration points were
361 included (*i.e.* Fig. 3c). The relevance to final methane concentrations is demonstrated by
362 considering the PAC2 samples reported by the University of Hawaii. A measured peak area of
363 62 for a sample volume of 0.076 L and a seawater density of 1024 kg m^{-3} , yields final methane
364 concentrations of 2.1, 2.2, and 2.8 nmol kg^{-1} depending on whether the equations from Fig.3a,
365 3b, or 3c are used, respectively. Therefore, an almost 30% increase in final methane
366 concentration results from use of the equation in Figure 3c, compared to Figure 3a. With this
367 understanding on the effect of FID calibration, we consider it likely that the increased deviation
368 from median values at high methane concentrations (Datasets B, C, and H) results from
369 differences in calibration slope between each laboratory. In contrast, the datasets with a higher
370 offset at low methane concentrations could be due to the use of incorrect intercepts as well as
371 other factors including sample contamination, discussed below (Datasets J and K).

372



373 3.3 Nitrous oxide concentrations in the intercomparison samples

374 Overall, median nitrous oxide concentrations in seawater samples collected from the Pacific
375 Ocean and the Baltic Sea ranged from 3.4 to 42.4 nmol kg⁻¹ (Table 2). Of the 113 reported
376 values, ten outliers were identified using the IQR criterion and were not included in further
377 analysis. The nitrous oxide data values for each batch of samples analyzed by each laboratory,
378 including the mean and standard deviation, the number of samples analyzed, and the % offset
379 from the overall median value are reported in Table S3 and Table S4 in the Supplement.

380 For six sets of seawater samples, BAL1, BAL2, BAL3, BAL6, BAL7, and PAC2, the
381 concentrations of nitrous oxide were close to atmospheric equilibrium. The reported values
382 ranged from 7.7 to 12.7 nmol kg⁻¹ in the Baltic Sea (Fig. 4a) and from 5.9 to 7.6 nmol kg⁻¹ in the
383 Pacific Ocean (Fig. 4b). For the Pacific Ocean near-surface sampling site (PAC2), the
384 theoretical value of nitrous oxide concentration in equilibrium with the overlying atmosphere is
385 also shown (Fig. 4b). For these six samples with concentrations close to atmospheric
386 equilibrium, the mean coefficient of variation for all laboratories ranged from 3% (BAL3 and
387 PAC2) to 5% (BAL1) (Table 2).

388 For the three other sets of samples (BAL4, BAL5, and PAC1), the nitrous oxide
389 concentrations deviated significantly from atmospheric equilibrium (Fig. 4c, 4d, and 4e). At one
390 sampling site, BAL4 (Fig. 4c), nitrous oxide was under-saturated with respect to atmospheric
391 equilibrium and reported concentrations ranged from 2.1–5.5 nmol kg⁻¹. As observed in the low
392 concentration Pacific Ocean methane samples, there was a skewed distribution of the data
393 towards the higher nitrous oxide concentrations. The BAL4 samples also had the highest
394 variability (*i.e.* lowest precision), with a mean coefficient of variation of 8% (Table 2). The two
395 remaining samples (PAC1 and BAL5) had much higher concentrations of nitrous oxide, as
396 expected for low-oxygen regions of the water-column. In contrast to the samples with near
397 atmospheric equilibrium concentrations of nitrous oxide, there was a low overall agreement
398 between the independent laboratories for PAC1 and BAL5 nitrous oxide concentrations (Fig. 4d,
399 4e). At PAC1 and BAL5, reported nitrous oxide concentrations ranged from 34.3–45.8 nmol kg⁻¹
400 (Fig. 4d) and 30.1–45.9 nmol kg⁻¹, respectively (Fig. 4e). The mean coefficient of variation for
401 all laboratories was 4% for BAL5 samples compared to 3% for PAC1 samples.

402 The deviation from median value was analyzed for the nitrous oxide datasets to gain a deeper
403 insight into the variability associated with their measurements (Fig. 5). The BAL1 dataset was



404 not included in this analysis due to its skewed data distribution and the high inter-laboratory
405 variability for BAL5 indicated that the median value may differ from the absolute nitrous oxide
406 concentration for this sample. For the low nitrous oxide Baltic Sea and Pacific Ocean samples
407 (Fig. 5a), the majority of data points were within 5% of the median values. Furthermore, for the
408 majority of laboratories, the data points for separate seawater samples clustered together
409 indicating some consistency to the extent they varied from the overall median value. Exceptions
410 to this observation include Datasets E, C, L, and K (Fig. 5a) which demonstrated varying
411 precision and accuracy. At high nitrous oxide concentrations (Fig. 5b), there are fewer data
412 points within 5% of the median value compared to low nitrous oxide concentrations (Fig. 5a).
413 Therefore, for PAC1 and BAL5 samples, 6 and 7 data points fall within 5% of the median value,
414 respectively. Furthermore, only three laboratories (Datasets F, G, and K) had data for both
415 Pacific Ocean and Baltic Sea samples within 5% of the median value. This could have been
416 caused by inconsistent analysis between different batches of samples or by variable sample
417 collection and transportation.

418 The likely factors that caused these offsets in nitrous oxide concentrations among
419 laboratories include sample analysis and calibration of the gas analyzers. Calibration of the ECD
420 is nontrivial and at least two prior publications have discussed nitrous oxide calibration issues
421 (Butler and Elkins, 1990; Bange et al., 2001). The laboratories participating in the nitrous oxide
422 intercomparison employed different calibration procedures (Fig. 6). Some used a linear fit and
423 maintained their analytical peak areas within a narrow range (Fig. 6a), while others used a step-
424 wise linear fit and therefore used different slopes for low and high nitrous oxide mole fractions
425 (Fig. 6b). Finally, some applied a polynomial curve (Fig. 6c) and sometimes two different
426 polynomial fits, for low and high concentrations. The difficulty in calibrating the ECD was
427 evidenced by the deviation from median values as multiple datasets show good precision but
428 consistent offsets at the lowest (Fig. 5a) and highest (Fig. 5b) final concentrations of nitrous
429 oxide.

430 **3.4 Sample storage**

431 Because prolonged sample storage adversely affects dissolved methane and nitrous oxide
432 samples (Magen et al., 2014), the intercomparison datasets were analyzed for sample storage
433 effects (Table S5 in the Supplement). It should however be noted that assessing the effect of
434 storage time on sample integrity was not a formal goal of the intercomparison exercise and



435 replicate samples were not analyzed at repeated intervals by independent laboratories, as would
436 normally be required for a thorough analysis. Nonetheless our results did provide some insights.
437 The comparison of measured concentrations (nmol kg^{-1}) and coefficients of variation (%) against
438 storage times revealed that low concentration methane samples (*i.e.* PAC1 and PAC2) were
439 susceptible to an increase in concentrations (Fig. 7a) and increased variability (Fig. 7b) with
440 increasing storage, as also observed by Magen et al. (2014). This was not as prevalent for higher
441 methane concentrations; however for samples with the highest methane concentrations *i.e.*
442 BAL5, there was some indication of a decrease in concentration with prolonged storage,
443 presumably as a result of gas leakage (Table S5 in the Supplement). For nitrous oxide, the
444 prominent observation was a potential decrease in concentration for higher concentration
445 seawater samples (*i.e.* BAL2), again presumably due to gas leakage. For low nitrous oxide
446 concentrations there was no comparable trend of increasing values to that observed for low
447 methane concentrations.

448

449 **4. Discussion**

450 The marine methane and nitrous oxide analytical community is growing. This is reflected in the
451 increasing number of corresponding scientific publications and the resulting development of a
452 global database for methane and nitrous oxide (Bange et al., 2009). Like all Earth observation
453 measurements, there is a need for intercomparison exercises of the type reported here, for data
454 quality assurance, and for appropriate reporting practices (National Research Council, 1993). To
455 the best of our knowledge, the work presented here is the first formal intercomparison of
456 dissolved methane and nitrous oxide measurements. Based on our results, we discuss the lessons
457 learned and our recommendations moving forward, by addressing the four questions that were
458 posed in the Introduction.

459

460 **4.1 What is the agreement between the SCOR gas standards and the ‘in-house’ gas** 461 **standards used by each laboratory?**

462 It is typical for laboratories to source some, or all, of their compressed gas standards from
463 commercial suppliers. National agencies, such as NOAA GMD or National Institute of
464 Metrology China, also provide standards to the scientific community. The national agencies
465 typically offer a lower range in concentrations than commercial suppliers, but their standards



466 tend to have a higher level of accuracy. Of the twelve laboratories participating in the
467 intercomparison, eight reported using national agency standards, with seven of them using gases
468 sourced from NOAA GMD. Since the methane and nitrous oxide mole fractions of these
469 national agency standards are equivalent to modern-day atmospheric mixing ratios, they are
470 similar to the SCOR ARS distributed to the majority of laboratories in this study. Laboratories
471 in receipt of the SCOR standards were asked to predict their mole fractions based on those of
472 their own in-house standards. For the majority that conducted this exercise, there was good
473 agreement (<3% difference) between the NOAA GMD and the SCOR ARS for both methane
474 and nitrous oxide. For three laboratories, a larger offset was observed between the NOAA GMD
475 and the SCOR ARS. There was also a good prediction for the higher methane content SCOR
476 WRS, facilitated by the linear response of the FID (Fig. 3). In contrast, the nitrous oxide mole
477 fraction in the SCOR WRS exceeded the typical working range for several laboratories and it
478 was difficult for them to cross-compare with their in-house standards. This reflects an analytical
479 set-up that involves on-column injection via a 6-port or 10-port valve with one or two sample
480 loops, respectively. The sample loops have a fixed volume and their inaccessibility makes it
481 difficult to replace them by a smaller loop size. Therefore either dilution of the standard is
482 required, or smaller loops need to be incorporated into the calibration protocol. The two
483 laboratories that compared their in-house standards with the SCOR WRS reported an offset of
484 3% and >20%. This indicates that variability between standards can be an issue for obtaining
485 accurate dissolved concentrations and provides support for the production of a widely available
486 high concentration nitrous oxide standard. We strongly recommend that all commercially
487 obtained standards are cross-checked against primary standards, such as the SCOR ARS and
488 WRS. This should be conducted at least at the beginning and end of their use to detect any drift
489 that may have occurred during their lifetime. With due diligence and care, the SCOR standards
490 provide the capability for cross-checking personal standards for years to decades (Bullister et al.,
491 2016).

492

493 **4.2 How do measured values of methane and nitrous oxide compare across laboratories?**

494 **Methane:** The methane intercomparison highlighted the variability that exists between
495 measurements conducted by independent laboratories. At low methane concentrations, a skewed
496 distribution of methane data was observed, which was particularly evident in PAC1 (Fig. 1a).



497 Potential causes include calibration procedures (Section 3.2) and/or sample contamination which
498 is more prevalent at low concentrations (Section 3.4). For some laboratories, the low methane
499 concentrations are close to their detection limit, which is determined by the relatively low
500 sensitivity of the FID and the small number of moles of methane in an introduced headspace
501 equilibration with seawater. An approximate working detection limit for methane analysis via
502 headspace equilibration is 1 nmol kg^{-1} , although some laboratories improve upon this by having
503 a large aqueous: gaseous phase ratio during the equilibration process (*e.g.* Upstill-Goddard et al.,
504 1996). Depending upon the volume of sample analyzed, purge-and-trap analysis can have a
505 detection limit much lower than 1 nmol kg^{-1} (*e.g.* Wilson et al., 2017). Methane measurements
506 in aquatic habitats with methane concentrations near the limit of analytical detection include
507 mesopelagic and high latitude environments distal from coastal or benthic inputs (Rehder et al.,
508 1999; Kitidis et al., 2010; Fenwick et al., 2017). Of additional concern is that the skewed
509 distribution of methane concentrations also occurs in samples collected both from the surface
510 ocean (PAC2; Fig. 1b) and coastal environments (BAL1; Fig. 1c). Methane concentrations
511 between $2\text{--}6 \text{ nmol kg}^{-1}$ are within the detection limit of all participating laboratories. To address
512 this we recommend that laboratories restrict sample storage to the minimum time required to
513 analyze the samples and incorporate internal controls into their sample analysis (Section 4.4).

514 There was an improvement in the overall agreement between the laboratories for samples
515 with higher methane concentrations. However, some of the highest variability between the
516 laboratories was observed at the highest concentrations of methane analyzed (BAL2; Fig. 1e).
517 This high degree of variability resulted in significant uncertainty in the absolute *in situ*
518 concentration. Methane concentrations of this magnitude and higher are found in coastal
519 environments (Zhang et al., 2004; Jakobs et al., 2014; Borges et al., 2017) and in the water-
520 column associated with seafloor emissions (*e.g.* Pohlman et al., 2011). These environments are
521 considered vulnerable to climate induced changes and eutrophication, and therefore it is
522 necessary that independent measurements are conducted to the highest possible accuracy to
523 allow for inter-laboratory and inter-habitat comparisons. To address this we recommend that
524 reference material be produced and distributed between laboratories.

525

526 **Nitrous oxide:** Some of the trends discussed for methane were also evident in the nitrous oxide
527 data. For the samples with the lowest nitrous oxide concentrations a skewed data distribution



528 was observed, as found for methane (Fig. 4c). Such low nitrous oxide concentrations are typical
529 of low-oxygen water-column environments ($<10 \mu\text{mol kg}^{-1}$). Therefore, the analytical bias
530 towards measuring values higher than the absolute *in situ* concentrations is particularly pertinent
531 to oceanographers measuring nitrous oxide in oxygen minimum zones and other low-oxygen
532 environments (Naqvi et al., 2010; Farías et al., 2015; Ji et al., 2015). The low concentrations of
533 nitrous oxide still exceed detection limits by at least an order of magnitude for even the less-
534 sensitive headspace method due to the high sensitivity of the ECD. Therefore, the bias towards
535 reporting elevated values for low concentrations of nitrous oxide is related less to analytical
536 sensitivity and is more a consequence of calibration issues. During the intercomparison exercise
537 ECD calibration was identified as a nontrivial issue for all participating laboratories and it
538 deserves continuing attention. In particular, the nonlinearity of the ECD means that low and
539 high nitrous oxide concentrations are more vulnerable to error since the values fall outside of the
540 most frequented part of the calibration curve. This is particularly true if a linear fit is used to
541 calibrate the ECD (Fig. 6a). To circumvent this problem, one laboratory used a step-wise linear
542 function while other laboratories used a quadratic function. The usefulness of multiple
543 calibration curves for low and high nitrous oxide concentrations was highlighted during the
544 intercomparison exercise, although this necessitates some consideration of the threshold for
545 switching different calibration curves.

546 The majority of seawater samples analyzed had nitrous oxide concentrations ranging from 7–
547 11 nmol kg^{-1} (Fig. 4a, 4b), which are close to atmospheric equilibrium values, as shown for the
548 Pacific Ocean (Fig. 4b). Collective analysis of these samples gives insight into the precision and
549 accuracy associated with surface water nitrous oxide analysis (Fig 5a). This is discussed further
550 in the context of implementing internal controls for methane and nitrous oxide (Section 4.4). For
551 samples with the highest nitrous oxide concentrations, *i.e.* exceeding 30 nmol kg^{-1} , there was
552 high variability between the concentrations reported by the independent laboratories. This was
553 most evident for the BAL5 samples (Fig. 4e) and similar to the variability observed at the highest
554 methane concentrations analyzed (Fig. 1e). It is difficult to assess how much of this variability
555 was specifically due to the differences in calibration practices between the laboratories and the
556 differences in gas standards with high nitrous oxide mole fractions, but at least some of it can be
557 attributed to this. These results form the basis for a proposed production of reference material
558 for both trace gases.



559

560 **4.3 Are there general recommendations to reduce uncertainty in the accuracy and**
561 **precision of methane and nitrous oxide measurements?**

562 Lessons learned during the intercomparison exercises will be the basis for a forthcoming Good
563 Practice Guide for dissolved methane and nitrous oxide. Key points include the use of traceable
564 gas standards (discussed in Section 4.1), calibration fits (discussed in Section 3.2 and 3.3),
565 sample storage time (discussed in Section 3.4), internal controls, and reference material.

566 Laboratories participating in this intercomparison exercise used one of two analytical
567 approaches; either headspace equilibration or the purge-and-trap technique. Aside from the low
568 methane concentrations, for some laboratories both analytical approaches yielded comparable
569 values for methane and nitrous oxide. At sub-nanomolar methane concentrations, four out of the
570 six laboratories that reported methane concentrations $<1 \text{ nmol kg}^{-1}$ used a purge-and-trap
571 analysis.

572 Internal controls represent a self-assessment quality control check to validate the analytical
573 method and quantify the magnitude of uncertainty. Appropriate internal controls for methane
574 and nitrous oxide consist of air-equilibrated seawater samples. Their purpose is to provide
575 checks for methane concentrations ranging from $2\text{--}3 \text{ nmol kg}^{-1}$ and for nitrous oxide
576 concentrations from $5\text{--}9 \text{ nmol kg}^{-1}$. The air used in the equilibration process could derive from
577 the ambient environment if sufficiently stable or from a compressed gas cylinder after cross-
578 checking the concentration with the appropriate gas standard. Air-equilibrated samples provide
579 reassurance that the analytical system is providing values within the correct range. Air-
580 equilibrated samples also indicate the certainty associated with calculating the saturation state of
581 the ocean with respect to atmospheric equilibrium. This is particularly relevant when the
582 seawater being sampled is within a few percent of saturation. Finally, these air-equilibrated
583 samples provide an estimate of analytical accuracy, which is infrequently reported for methane
584 or nitrous oxide. At present, only a few studies report the analysis of air-equilibrated seawater
585 alongside water-column samples (Bullister and Wisegarver, 2008; Capelle et al., 2015; Wilson et
586 al., 2017). It is considered likely that wider implementation would facilitate internal assessment
587 of the analytical system. Since the main equipment required is a water-bath and an overhead
588 stirrer, the production is not cost-prohibitive. A recommendation of this intercomparison



589 exercise is that laboratories routinely use air-equilibrated seawater samples to provide an
590 estimate of analytical accuracy.

591 In addition to the self-assessments provided by the analysis of air-equilibrated seawater, this
592 study revealed the need for reference seawater to help assess the accuracy of high concentration
593 methane and nitrous oxide measurements. Reference seawater in this instance refers to batches
594 of dissolved methane and nitrous oxide samples prepared in the laboratory using an equilibrator
595 set-up, as used for dissolved inorganic carbon (Dickson et al., 2007). In the absence of plans for
596 additional intercomparison exercises, the provision of reference seawater will allow laboratories
597 to continue evaluating their own measurements.

598

599 **4.4 What are the implications of interlaboratory differences for determining the spatial and** 600 **temporal variability of methane and nitrous oxide in the oceans?**

601 The key outcome of this study was the identification of differences in methane and nitrous oxide
602 concentrations for the same batch of seawater samples measured by several independent
603 laboratories. Emergent from this is the distinct possibility that any given laboratory will
604 incorrectly report data, thereby increasing uncertainty over the saturation states of both gases.

605 The tendency to over-estimate methane concentrations close to atmospheric equilibrium means
606 that marine emissions of methane to the overlying atmosphere will be also overestimated (Bange
607 et al., 1994; Upstill-Goddard and Barnes, 2016). In contrast, for nitrous oxide there does not
608 appear to be either an under-estimation or over-estimation of concentrations. Consequently, there
609 is generally a lower inherent uncertainty in its surface ocean saturation state, as previously
610 proposed (Law and Ling, 2001; Forster et al., 2009).

611 The inter-laboratory differences highlighted by this study should be viewed in the context of
612 numerous individual efforts to assess temporal and/or spatial trends in methane and nitrous oxide
613 by way of time-series observations (Bange et al., 2010; Farías et al., 2015; Wilson et al., 2017;
614 Fenwick and Tortell, 2018), repeat hydrographic survey lines (de la Paz et al., 2017), and single
615 expeditions. While the value of these in integrating the behaviour of methane and nitrous oxide
616 into the hydrography and biogeochemistry of local-regional ecosystems is beyond question, their
617 value would be enhanced by the rigorous cross-validation of analytical protocols. Without this,
618 perceived small temporal and/or spatial changes in water-column concentrations in any given
619 region are difficult to verify unless the data all originate from a single laboratory. In addition,



620 the value of a global methane and nitrous oxide database (*e.g* Bange et al., 2009) would to some
621 extent be compromised by the uncertainty. Taking due account of the analytical variability
622 between laboratories will clearly be vital to any future assessment of the changing methane and
623 nitrous oxide budgets of the oceans.

624

625 **5. Conclusions**

626 Overall, the intercomparison exercise was invaluable to the growing community of oceanic
627 methane and nitrous oxide analysts. The level of agreement between independent measurements
628 of dissolved concentrations was evaluated in the context of several contributing factors,
629 including sample analysis, standards, calibration procedures, and sample storage time.
630 Importantly, the intercomparison represents a concerted effort from the scientists involved to
631 critically assess the quality of their data, and to initiate the steps required for further
632 improvements. Recommendations arising from the intercomparison include routine cross-
633 calibration of working gas standards against primary standards, minimizing sample storage time,
634 incorporating internal controls (air-equilibrated seawater) alongside routine sample analysis, and
635 the future production of reference seawater for methane and nitrous oxide measurements. These
636 efforts will help resolve temporal and spatial variability, which is necessary for constraining
637 methane and nitrous oxide emissions from aquatic ecosystems and for evaluating the processes
638 that govern their production and consumption in the water-column.



639 *Acknowledgements:* The methane and nitrous oxide intercomparison exercise was conducted as a
640 Scientific Committee on Ocean Research (SCOR) Working Group which receives funding from
641 the U.S. National Science Foundation (OCE-1546580). Pacific Ocean seawater samples were
642 collected on HOT cruises which are supported by NSF (including the most recent OCE-1260164
643 to DMK). Baltic Sea seawater samples were collected during Cruise #142 of the RV Elisabeth
644 Mann Borgese, with the ship-time provided by the Leibniz Institute for Baltic Sea Research
645 Warnemünde. We thank Liguu Guo for help with sampling during the Baltic Sea cruise. The
646 methane and nitrous oxide gas standards were produced via a Memorandum of Understanding
647 between the University of Hawaii and NOAA-PMEL. Funding for the gas standards was
648 provided by for the Center for Microbial Oceanography: Research and Education (C-MORE;
649 EF0424599 to DMK), SCOR, the EU FP7 funded Integrated non-CO₂ Greenhouse gas
650 Observation System (InGOS) (Grant Agreement #284274), and NOAA's Climate Program
651 Office, Climate Observations Division. Additional support was provided by the Gordon and
652 Betty Moore Foundation #3794 (DMK), the Simons Collaboration on Ocean Processes and
653 Ecology (SCOPE; #329108 to DMK), and the Global Research Laboratory Program (#
654 2013K1A1A2A02078278 to DMK) through the National Research Foundation of Korea (NRF).
655 AVB is a senior research associate at the FRS-FNRS. AES would like to acknowledge NSF
656 OCE-1437310. MP would like to acknowledge the support of the Spanish Ministry of Economy
657 and Competitiveness (CTM2015-74510-JIN). Any use of trade names is for descriptive
658 purposes and does not imply endorsement by the U.S. government



659 **References**

- 660 Anderson, B., Bartlett, K., Frolking, S., Hayhoe, K., Jenkins, J., and Salas, W.: Methane and
661 nitrous oxide emissions from natural sources, Office of Atmospheric Programs, US EPA,
662 EPA 430-R-10-001, Washington DC, 2010.
- 663 Arévalo-Martínez, D. L., Beyer, M., Krumbholz, M., Piller, I., Kock, A., Steinhoff, T.,
664 Körtzinger, A., and Bange, H. W.: A new method for continuous measurements of oceanic
665 and atmospheric N₂O, CO and CO₂: performance of off-axis integrated cavity output
666 spectroscopy (OA-ICOS) coupled to non-dispersive infrared detection (NDIR), *Ocean Sci.*,
667 9, 1071–1087, 2013.
- 668 Atkinson, L. P., and Richards, F. A.: The occurrence and distribution of methane in the marine
669 environment, *Deep-Sea Res.*, 14, 673–684, 1967.
- 670 Bange, H. W., Bartell, U. H., Rapsomanikis, S., and Andreae, M. O.: Methane in the Baltic and
671 North Seas and a reassessment of the marine emissions of methane, *Global Biogeochem.*
672 *Cycles*, 8, 465–480, doi:10.1029/94GB02181, 1994.
- 673 Bange, H. W., Rapsomanikis, S., and Andreae, M. O.: Nitrous oxide cycling in the Arabian Sea,
674 *J. Geophys. Res.: Oceans*, 106, 1053–1065, 2001.
- 675 Bange H.W, Bell, T.G., Cornejo, M., Freing, A., Uher, G., Upstill-Goddard, R.C., and Zhang G.
676 MEMENTO: a proposal to develop a database of marine nitrous oxide and methane
677 measurements. *Env. Chem*, 6, 195–197, 2009.
- 678 Bange, H.W., Bergmann, K., Hansen, H.P., Kock, A., Koppe, R., Malien, F., and Ostrau, C.:
679 Dissolved methane during hypoxic events at the Boknis Eck Time Series Station
680 (Eckernförde Bay, SW Baltic Sea), *Biogeosci.*, 7, 1279–1284, 2010.
- 681 Borges, A.V., Speeckaert, G., Champenois, W., Scranton, M.I., and Gypens, N.: Productivity and
682 temperature as drivers of seasonal and spatial variations of dissolved methane in the Southern
683 Bight of the North Sea, *Ecosystems*, 1–17, 2017.
- 684 Bullister, J. L., Wisegarver, D. P., and Menzia, F. A.: The solubility of sulfur hexafluoride in
685 water and seawater, *Deep-Sea Res.*, 49, 175–187, 2002.
- 686 Bullister, J. L., and Wisegarver, D. P.: The shipboard analysis of trace levels of sulfur
687 hexafluoride, chlorofluorocarbon-11 and chlorofluorocarbon-12 in seawater, *Deep-Sea Res.*,
688 55, 1063–1074, 2008.
- 689 Bullister, J. L., and Tanhua, T.: Sampling and measurement of chlorofluorocarbons and sulfur
690 hexafluoride in seawater, IOCCP Report No. 14 ICPO Publication Series No. 134, Version 1,
691 2010.



- 692 Bullister, J. L., Wisegarver, D. P., and Wilson, S. T.: The production of methane and nitrous
693 oxide gas standards for Scientific Committee on Ocean Research (SCOR) Working Group
694 #143, <http://www.scor-int.org/Publications>, 2016.
- 695 Butler, J. H., Elkins, J. W., Thompson, T. M., and Egan, K. B.: Tropospheric and dissolved N₂O
696 of the west Pacific and east Indian Oceans during the El Nino Southern Oscillation Event of
697 1987, *J. Geophys. Res.*, 94, 14,865–14,877, 1989.
- 698 Butler, J. H., and Elkins, J. W.: An automated technique for the measurement of dissolved N₂O
699 in natural waters, *Mar. Chem.*, 34, 47–61, 1991.
- 700 Capelle, D. W., Dacey, J. W., and Tortell, P. D.: An automated, high through-put method for
701 accurate and precise measurements of dissolved nitrous oxide and methane concentrations in
702 natural waters, *Limnol. Oceanogr.: Methods*, 13, 345–355, 2015.
- 703 Ciais, P., Dolman, A.J., Bombelli, A., Duren, R., Peregon, A., Rayner, P.J., Miller, C., Gobron,
704 N., Kinderman, G., Marland, G., and Gruber, N.: Current systematic carbon-cycle
705 observations and the need for implementing a policy-relevant carbon observing system,
706 *Biogeosciences*, 11, 3547–3602, 2014.
- 707 Craig, H. and Gordon, L. I.: Nitrous oxide in the ocean and the marine atmosphere, *Geochim.*
708 *Cosmochim. Acta* 27, 949–955, 1963.
- 709 Cutter, G. A.: Intercalibration in chemical oceanography - getting the right number. *Limnol.*
710 *Oceanogr.: Methods*, 11, 418–424, 2013.
- 711 de la Paz, M., García-Ibáñez, M.I., Steinfeldt, R., Ríos, A.F., and Pérez, F.F.: Ventilation versus
712 biology: What is the controlling mechanism of nitrous oxide distribution in the North
713 Atlantic?, *Global Biogeochem. Cy.*, 31, 745–760, doi: 10.1002/2016GB005507, 2017.
- 714 Dickson, A. G., Sabine, C. L. and Christian, J. R.: Guide to best practices for ocean CO₂
715 measurements, PICES Special Publication 3, 2007.
- 716 Farías, L., Castro-González, M., Cornejo, M., Charpentier, J., Faúndez, J., Boontanon, N. and
717 Yoshida, N.: Denitrification and nitrous oxide cycling within the upper oxycline of the
718 eastern tropical South Pacific oxygen minimum zone. *Limnol. Oceanogr.*, 54, 132–144,
719 2009.
- 720 Farías, L., Besoain, V., and García-Loyola, S.: Presence of nitrous oxide hotspots in the coastal
721 upwelling area off central Chile: an analysis of temporal variability based on ten years of a
722 biogeochemical time series, *Environ. Res. Lett.*, 10, 044017, 2015.
- 723 Fenwick, L., and Tortell, P. D.: Methane and nitrous oxide distributions in coastal and open
724 ocean waters of the Northeast Subarctic Pacific during 2015–2016, *Mar. Chem.*, 200, 45–56,
725 2018.



- 726 Fenwick, L., Capelle, D., Damm, E., Zimmermann, S., Williams, W. J., Vagle, S., and Tortell, P.
727 D.: Methane and nitrous oxide distributions across the North American Arctic Ocean during
728 summer, 2015, *J. Geophys. Res.: Oceans*, 122, 390–412, doi:10.1002/2016JC012493, 2017.
- 729 Forster, G., Upstill-Goddard, R. C., Gist, N., Robinson, C., Uher, G. and Woodward, E. M. S.:
730 Nitrous oxide and methane in the Atlantic Ocean between 50 N and 52 S: latitudinal
731 distribution and sea-to-air flux, *Deep-Sea Res.*, 56, 964–976, 2009.
- 732 Freing, A., Wallace, D. W. R., and Bange, H. W.: Global oceanic production of nitrous oxide,
733 *Phil. Trans. R. Soc. B*, 367, 1245–1255, 2012.
- 734 Gülzow, W., Rehder, G., Schneider, B., Schneider, J., Deimling, V., and Sadkowiak, B.: A new
735 method for continuous measurement of methane and carbon dioxide in surface waters using
736 off-axis integrated cavity output spectroscopy (ICOS): An example from the Baltic Sea,
737 *Limnol. Oceanogr.: Methods*, 9, 176–184, 2011.
- 738 Jakobs, G., Holterman, P., Berndmeyer, C., Rehder, G., Blumenberg, M., Jost, G., Nausch, G.,
739 and Schmale, O.: Seasonal and spatial methane dynamics in the water column of the central
740 Baltic Sea (Gotland Sea), *Continental Shelf Res.*, 91, 12–25, 2014.
- 741 Ji, Q., Babbin, A. R., Jayakumar, A., Oleynik, S., and Ward, B. B.: Nitrous oxide production by
742 nitrification and denitrification in the Eastern Tropical South Pacific oxygen minimum zone,
743 *Geophys. Res. Lett.*, 42, 10,755–10,764, doi:10.1002/2015GL066853, 2015.
- 744 Kitidis, A., Upstill-Goddard, R. C., and Anderson, L. G.: Methane and nitrous oxide in surface
745 water along the North-West Passage, Arctic Ocean, *Mar. Chem.*, 121, 80–86, 2010.
- 746 Law, C. S., and Ling, R. D.: Nitrous oxide flux and response to increased iron availability in the
747 Antarctic Circumpolar Current, *Deep-Sea Res.*, 48, 2509–2527, 2001.
- 748 Magen, C., Lapham, L. L., Pohlman, J. W., Marshall, K., Bosman, S., Casso, M., and Chanton, J.
749 P.: A simple headspace equilibration method for measuring dissolved methane, *Limnol.*
750 *Oceanogr.: Methods*, 12, 637–650, 2014.
- 751 McAuliffe, C.: Solubility on water of C₁-C₉ hydrocarbons, *Nature*, 200, 1092–1093, 1963.
- 752 Myhre, G., Shindell, D., Bréon, F.-M., Collins, W., Fuglestedt, J., Huang, J., Koch, D.,
753 Lamarque, J.-F., Lee, D., Mendoza, B., Nakajima, T., Robock, A., Stephens, G., Takemura,
754 T., and Zhang, H.: Anthropogenic and Natural Radiative Forcing, In: *Climate Change 2013:
755 The Physical Science Basis. Contribution of Working Group I to the Fifth Assessment Report
756 of the Intergovernmental Panel on Climate Change* [Stocker, T. F., Qin, D., Plattner, G.-K.,
757 Tignor, M., Allen, S. K., Boschung, J., Nauels, A., Xia, Y., Bex, V., and Midgley, P. M.
758 (eds.)]. Cambridge University Press, Cambridge, United Kingdom and New York, NY, USA,
759 2013.



- 760 Naqvi, S. W. A., Bange, H. W., Farías, L., Monteiro, P. M. S., Scranton, M. I., and Zhang, J.:
761 Marine hypoxia/anoxia as a source of CH₄ and N₂O, *Biogeosciences*, 7, 215–2190, doi:
762 10.5194/bg-7-2159-2010, 2010.
- 763 National Research Council: Applications of analytical chemistry to oceanic carbon cycle studies.
764 Washington DC. National Academy Press, 1993.
- 765 Nevison, C. D., Weiss, R. F., and Erickson, D. J.: Global oceanic emissions of nitrous oxide, J.
766 *Geophys. Res.*, 100, 15809–15820, doi: 10.1029/95JC00684, 1995.
- 767 Pohlman, J. W., Bauer, J. E., Waite, W. F., Osburn, C. L., and Chapman, N. R.: Methane
768 hydrate-bearing seeps as a source of aged dissolved organic carbon to the oceans, *Nature*
769 *Geosci.*, 4, 37–41, 2011
- 770 Reeburgh, W. S.: Oceanic methane biogeochemistry, *Chem. Rev.*, 107, 486–513, doi:
771 10.1021/cr050362v, 2007.
- 772 Rehder, G., Keir, R. S., Suess, E., and Rhein, M.: Methane in the northern Atlantic controlled by
773 microbial oxidation and atmospheric history, *Geophys. Res. Lett.*, 26, 587–590, doi:
774 10.1029/1999GL900049, 1999.
- 775 Schmale, O., Schneider von Deimling, J., Gülzow, W., Nausch, G., Waniek, J. J. and Rehder, G.:
776 Distribution of methane in the water column of the Baltic Sea. *Geophys. Res. Lett.*, 37,
777 L12604, doi: 10.1029/2010GL043115, 2010.
- 778 Strady, E., Pohl, C., Yakushev, E. V., Krügera, S., and Hennings, U.: PUMP–CTD-System for
779 trace metal sampling with a high vertical resolution. A test in the Gotland Basin, Baltic Sea,
780 *Chemosphere*, 70, 1309–1319, 2008.
- 781 Swan, H. B., Armishaw, P., Iavetz, R., Alamgir, M., Davies, S. R., Bell, T. G., and Jones, G. B.:
782 An interlaboratory comparison for the quantification of aqueous dimethylsulfide. *Limnol.*
783 *Oceanogr.: Methods*, 12, 784–794, 2014.
- 784 Upstill-Goddard, R. C., Rees, A. P., and Owens, N. J. P.: Simultaneous high-precision
785 measurements of methane and nitrous oxide in water and seawater by single phase
786 equilibration gas chromatography, *Deep-Sea Res.*, 43, 1669–1682, 1996.
- 787 Upstill-Goddard, R. C., and Barnes, J.: Methane emissions from UK estuaries: Re-evaluating the
788 estuarine source of tropospheric methane from Europe, *Mar. Chem.*, 180, 14–23, 2016.
- 789 Walter, S., Peeken, I., Lochte, K., Webb, A., and Bange, H. W.: Nitrous oxide measurements
790 during EIFEX, the European Iron Fertilization Experiment in the subpolar South Atlantic
791 Ocean, *Geophys. Res. Letts*, 32, doi:10.1029/2005GL024619, 2005.



- 792 Weiss, R. F., and Price, B. A.: Nitrous oxide solubility in water and seawater, *Mar. Chem.*, 8,
793 347–359, doi: 10.1016/0304-4203(80)90024-9, 1980.
- 794 Weiss, R. F., Van Woy, F. A., and Salameh, P. K.: Surface water and atmospheric carbon
795 dioxide and nitrous oxide observation by shipboard automated gas chromatography: Results
796 from expeditions between 1977 and 1990, Scripps Institution of oceanography Reference 92-
797 11. ORNL/CDIAC-59, NDP-044. Carbon Dioxide Information Analysis Center, Oak Ridge
798 National Laboratory, Tennessee, 1992.
- 799 Wiesenburg, D. A., and Guinasso, N. L.: Equilibrium solubilities of methane, carbon monoxide
800 and hydrogen in water and seawater, *J. Chem. Eng. Data*, 24, 354–360, doi:
801 10.1021/je60083a006, 1979.
- 802 Wilson, S. T., Ferrón, S., and Karl, D. M.: Interannual variability of methane and nitrous oxide in
803 the North Pacific Subtropical Gyre, *Geophys. Res. Lett.*, 44, doi: 10.1002/2017GL074458,
804 2017.
- 805 Zhang, G. L., Zhang, J., Kang, Y. B., and Liu, S. M.: Distributions and fluxes of methane in the
806 East China Sea and the Yellow Sea in spring, *J. Geophys. Res.*, 109, C07011,
807 doi:10.1029/2004JC002268, 2004



808 **Table 1.** List of laboratories that participated in the intercomparison. All laboratories measured
 809 both methane and nitrous oxide except U.S. Geological Survey (methane only), UCSB (nitrous
 810 oxide only), and NOAA PMEL (nitrous oxide from the Pacific Ocean). Also indicated are the
 811 twelve laboratories that received the SCOR gas standards of methane and nitrous oxide.

Institution	Lead Scientist	SCOR Standards
University of Hawaii, USA	Samuel Wilson	Yes
GEOMAR, Germany	Hermann Bange	Yes
Newcastle University, UK	Robert Upstill-Goddard	Yes
Université de Liège, Belgium	Alberto Vieira Borges	No
Plymouth Marine Laboratory, UK	Andrew Rees	Yes
NOAA PMEL, USA	John Bullister	Yes
IIM-CSIC, Spain	Mercedes de la Paz	Yes
CACYTMAR, Spain	Macarena Burgos	No
University of Concepción, Chile	Laura Farías	Yes
IOW, Germany	Gregor Rehder	Yes
University of California Santa Barbara, USA	Alyson Santoro	Yes
National Institute of Water and Atmospheric Research, NZ	Cliff Law	Yes
University British Columbia, Canada	Philippe Tortell	Yes
USGS, USA	John Pohlman	No
Ocean University of China, China	Guiling Zhang	Yes

812

813



814 **Table 2.** Pertinent information for each batch of methane and nitrous oxide samples. This
 815 includes contextual hydrographic information, median and mean concentrations of methane and
 816 nitrous oxide, range, number of outliers, and the overall average coefficient of variation (%).
 817

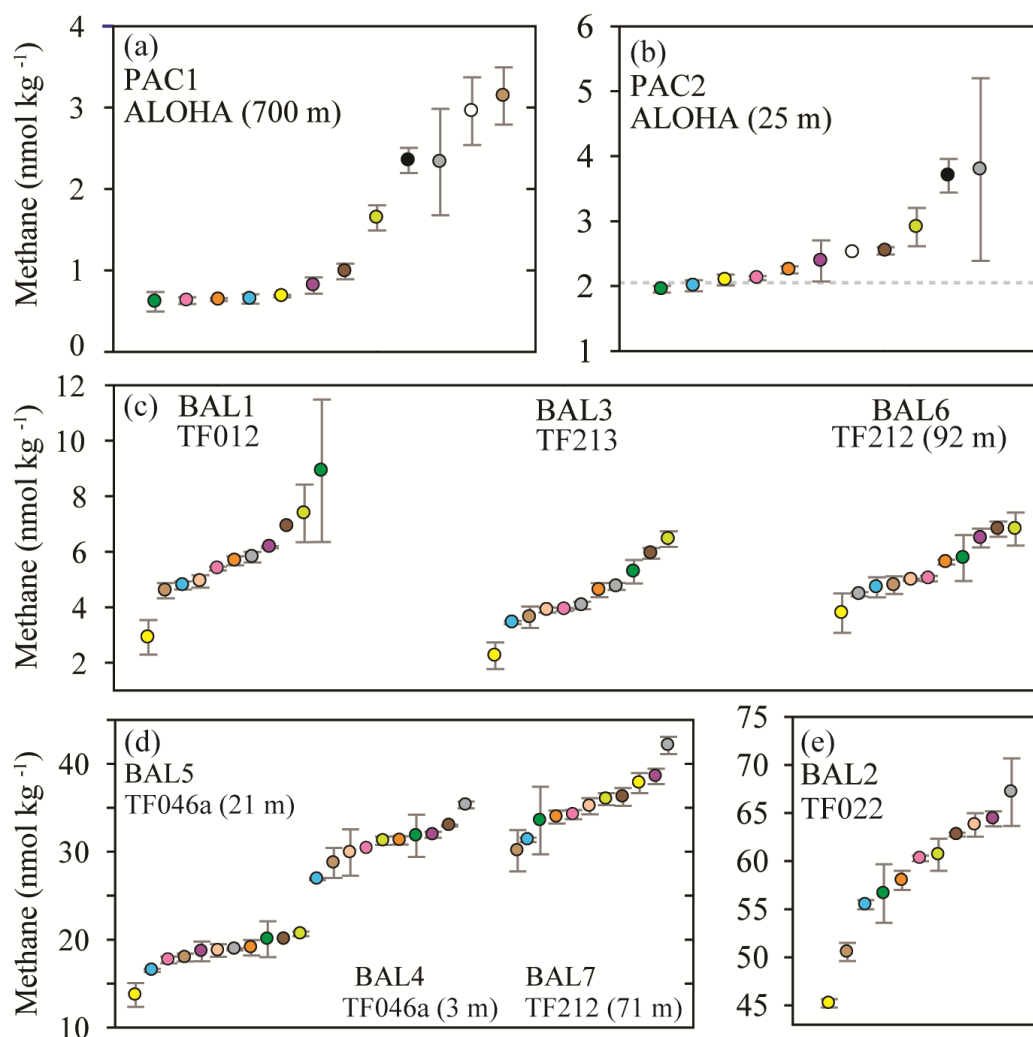
Sampling parameters									
Sample ID	PAC1	PAC 2	BAL1	BAL2	BAL3	BAL4	BAL5	BAL6	BAL7
Location	22.75N 158.00W	22.75N 158.00W	54.32N 11.55E	54.11N 11.18E	55.25N 15.98E	55.30N 15.80E	55.30N 15.80E	54.47N 12.21E	54.47N 12.21E
Location name	Station ALOHA	Station ALOHA	TF012	TF022	TF213	TF212	TF212	TF046a	TF046a
Sampling date	24.2.17	24.2.17	16.10.16	17.10.16	18.10.16	19.10.16	20.10.16	21.10.16	21.10.16
Sampling depth (m)	25	700	3	22	3	92	71	3	21
Seawater temperature (°C)	23.6	5.1	12.0	13.6	12.2	6.6	6.7	11.8	13.4
Salinity	34.97	34.23	13.85	17.37	7.87	18.40	18.08	8.81	17.65
Density (kg m ⁻³)	1024	1027	1010	1013	1006	1014	1014	1006	1013
Nitrous oxide									
Number of datasets	13	13	12	13	12	13	12	13	12
Outliers	0	1	2	1	1	0	1	2	2
Median N ₂ O conc. (nmol kg ⁻¹)	42.4	7.0	11.0	9.4	11.1	3.4	40.2	11.0	9.6
Mean N ₂ O conc. (nmol kg ⁻¹)	41.3	7.0	11.1	9.2	11.0	3.4	39.0	10.8	9.5
Range	34.3-45.8	5.9-7.6	10.1-12.7	7.7-11.0	9.6-11.6	2.1-5.5	30.1-45.9	9.5-11.5	8.0-10.4
Average coeff. variation (%)	2.8	4.4	4.5	4.2	2.7	7.5	4.0	2.6	4.4
Methane									
Number of datasets	12	12	11	11	11	11	11	11	11
Outliers	0	1	0	0	0	1	1	0	0
Median CH ₄ conc. (nmol kg ⁻¹)	0.9	2.3	5.7	60.3	4.1	31.3	18.8	5.0	35.2
Mean CH ₄ conc. (nmol kg ⁻¹)	1.8	2.6	5.8	58.6	4.4	31.1	18.8	5.4	35.4
Range	0.6-3.1	1.9-3.8	2.9-8.9	45.2-67.2	2.5-6.5	26.9-35.3	16.5-20.7	3.8-6.8	30.1-42.1
Average coeff. variation (%)	10.9	7.2	8.6	2.1	4.3	3.5	4.2	6.5	3.5

818

819

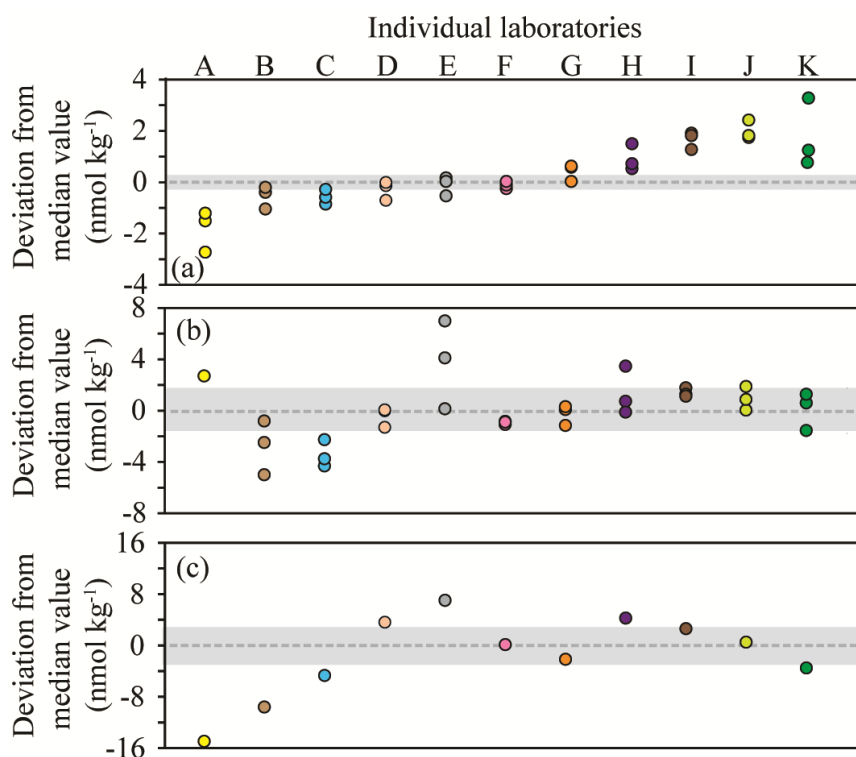


820 **Figures**



821
822
823
824
825
826
827
828
829

Figure 1. Concentrations of methane measured in nine separate seawater samples collected from the Pacific Ocean (Fig. 1a, 1b) and the Baltic Sea (Fig. 1c, 1d, 1e). The dashed grey line represents the value of methane at atmospheric equilibrium (Fig. 1b.) Individual data points are plotted sequentially in increasing value with the same color symbol for each laboratory in all plots.



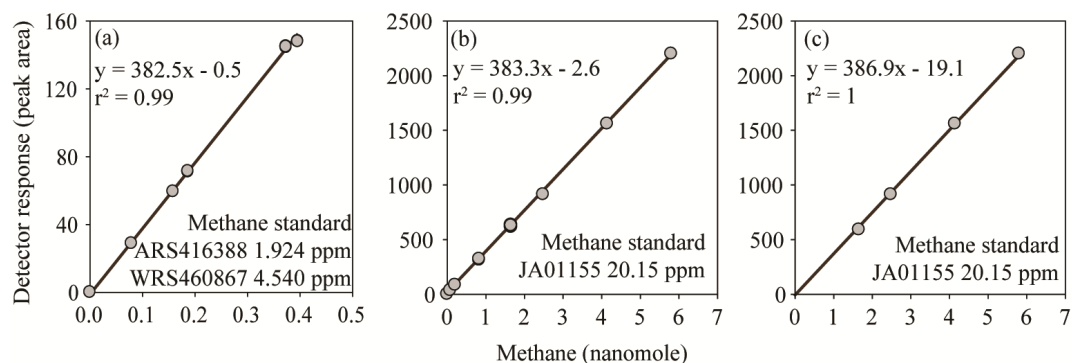
830

831 Figure 2. Deviation from the median methane concentration (reported as absolute values in nmol kg^{-1}) for the seven Baltic Sea samples. The batches of seawater samples include BAL1, BAL3, and BAL6 (Fig. 2a), BAL4, BAL5, and BAL7 (Fig. 2b), and BAL2 (Fig. 2c). The shaded grey area indicates values $\leq 5\%$ of the median concentration. The color scheme for each laboratory dataset is identical to that used in Figure 1 and the letters allocated to each dataset are to facilitate cross-referencing in the text. Note that the y-axis scale varies between the Figures.

837



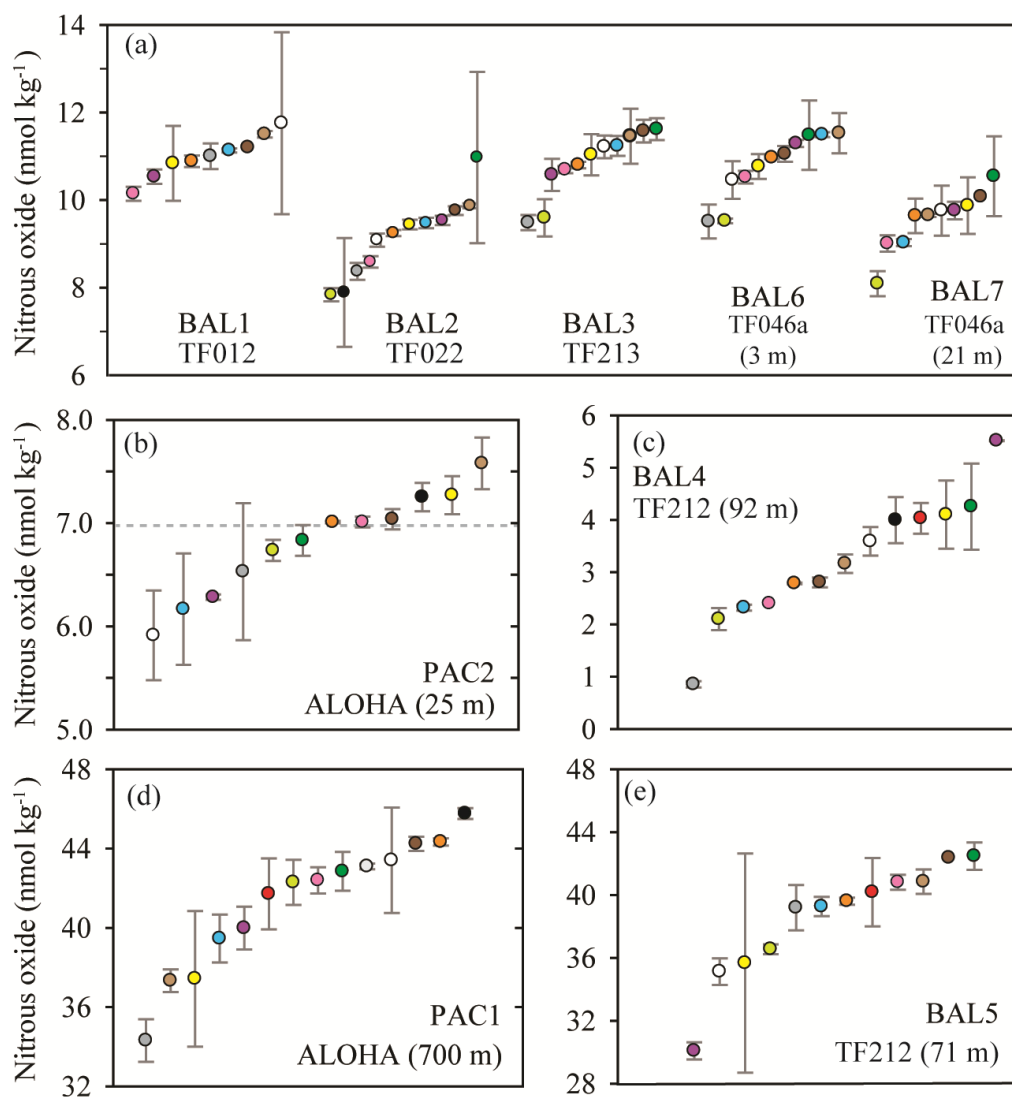
838



839

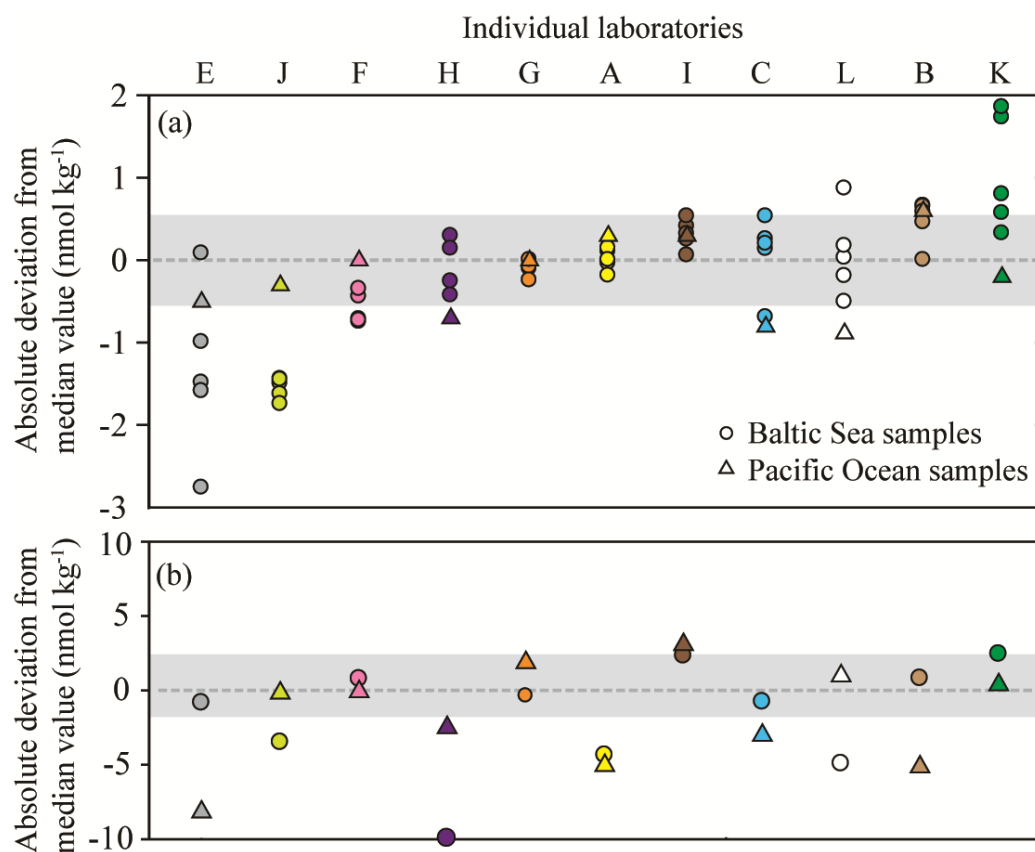
840 Figure 3. FID response to methane, fitted with a linear regression calibration. The inclusion
 841 (Fig. 3a and Fig. 3b) or exclusion (Fig. 3c) of low methane values cause the calibration slope and
 842 intercept to vary. However, the observed variation in the calibration slope does not have a
 843 significant effect on the final calculated concentrations of methane. In contrast, variation in the
 844 intercept does have an effect on the final concentrations of methane.

845



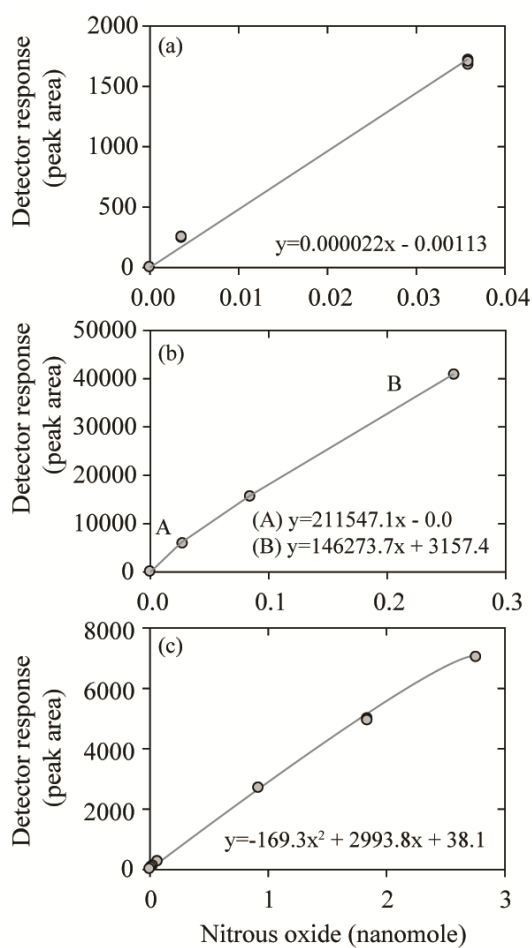
846
847
848
849
850
851
852

Figure 4. Concentrations of nitrous oxide measured in nine separate samples from the Baltic Sea and the Pacific Ocean. The dashed grey line represents the value of nitrous oxide at atmospheric equilibrium (Fig. 4b). Individual data points are plotted sequentially in increasing value with the same color symbol for each laboratory in all plots.



853
854

855 Figure 5. Deviation from the median value (reported in absolute units) for nitrous oxide datasets.
856 The batches of samples include BAL1,2,3,6,7 (Fig. 5a) and PAC2 and BAL5 (Fig. 5b). The
857 Baltic Sea samples are represented by circles and the Pacific Ocean samples are represented by
858 triangles. The shaded area indicates values $\leq 5\%$ based on a water-column concentration of 11
859 nmol kg^{-1} and 42 nmol kg^{-1} for Fig. 5a and 5b, respectively. The color scheme for each
860 laboratory dataset is identical to that used in Figure 4 and the letters allocated to each dataset are
861 to facilitate cross-referencing in the text. Note the y-axis for Fig 5a and 5b are plotted on a
862 different scale.

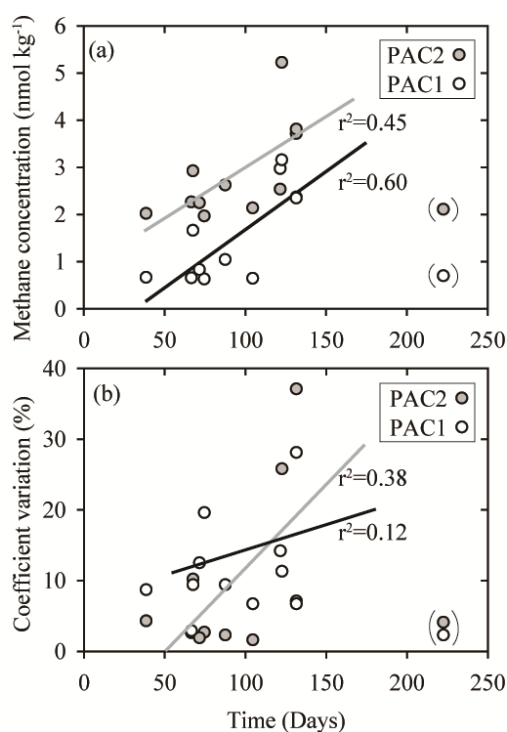


863

864 Figure 6. Three calibrations curves for nitrous oxide measurements using an ECD including
865 linear (Fig. 6a), multilinear (Fig. 6b), and quadratic (Fig. 6c).



866



867

868 Figure 7. Comparison of sample storage times with measured concentrations of methane (Fig.

869 7a) and coefficient variation (Fig. 7b) for two sets of seawater samples (PAC1 and PAC2).

870 These two sets of seawater samples had the lowest methane concentrations and appear to be

871 influenced by the duration of storage time. The data points enclosed in parentheses were not

872 included in the regression analysis. The PAC1 regression line is black and the PAC2 regression

873 line is grey. All of the storage times are included in the Supplementary Material.